Evidence for Cortical Functional Changes in Patients With Migraine and White Matter Abnormalities on Conventional and Diffusion Tensor Magnetic Resonance Imaging

Maria A. Rocca, MD; Bruno Colombo, MD; Elisabetta Pagani, PhD; Andrea Falini, MD; Maria Codella, MD; Giuseppe Scotti, MD; Giancarlo Comi, MD; Massimo Filippi, MD

Background—In this study, we used functional MRI (fMRI) to investigate the pattern of cortical activations after a simple motor task in patients with migraine and white matter (WM) abnormalities on conventional MRI scans of the brain. We also investigated whether the extent of brain activations was correlated with WM structural pathology measured using diffusion tensor (DT) MRI.

Methods—From 15 right-handed patients with migraine and 15 sex- and age-matched, right-handed healthy volunteers, we obtained the following: (1) fMRI (repetitive flexion-extension of the last 4 fingers of the right hand), (2) dual-echo turbo spin echo scans, and (3) pulsed-gradient spin-echo echo-planar sequence to calculate DT-MRI maps. fMRI analysis was performed using SPM99 and cluster detection. We measured the volume, the average mean diffusivity ($\bar{D}$), and the average fractional anisotropy of all lesions seen on the dual-echo scans. $\bar{D}$ histograms of the normal-appearing WM were also produced.

Results—Compared with healthy volunteers, migraine patients had a larger relative activation of the contralateral primary sensorimotor cortex ($P=0.01$) and a rostral displacement of the supplementary motor area ($P=0.03$). The shapes of the curves reflecting the time course for fMRI signal intensity changes were similar between migraine patients and controls for all of the cortical areas we studied. Compared with healthy subjects, migraine patients had significantly lower $\bar{D}$ histogram peak height of the normal-appearing WM histogram ($P=0.02$), which was found to be correlated with the extent of displacement of the supplementary motor area ($r=-0.80$, $P<0.001$).

Conclusions—This study suggests that functional cortical changes occur in patients with migraine and brain MRI abnormalities and that they might be secondary to the extent of subcortical structural damage. **(*Stroke*. 2003;34:665-670.)**

Key Words: diffusion tensor imaging ■ magnetic resonance imaging, functional ■ migraine

Several studies have shown the presence of white matter abnormalities on T_2-weighted MRI scans of the brain from patients with migraine,[1–11] which are likely to be the consequence of ischemic damage secondary to the repeated regional blood flow reductions known to occur during headache attacks.[11–15]

Functional MRI (fMRI) offers noninvasive access to the neuronal mechanisms of central nervous system functioning, and it is increasingly being used to define abnormal patterns of brain activations arising from various diseases.[16–25] In this context, recent work has shown that functional cortical changes, with the potential to limit the clinical consequences of the subcortical brain injury, can occur in multiple sclerosis (MS) patients with relatively few white matter lesions and modest or even no clinical symptomatology.[20,22–25]

Against this background, we performed the present study to investigate whether functional cortical changes are detectable in patients with migraine and subcortical white matter lesions as seen on conventional MRI scans. Given the known sensitivity of diffusion tensor (DT) MRI for the detection of ischemic tissue changes beyond the resolution of conventional scanning,[26–28] we also quantified the extent of normal-appearing white matter (NAWM) damage in these patients. The extent of structural tissue damage on conventional MRI and DT-MRI was then correlated with the extent of brain functional activations to assess whether fMRI changes might have an adaptive role in patients with migraine, as suggested for other white matter diseases.[20,22–25]

Patients and Methods

Patients

We studied 15 right-handed patients with migraine. The patients were recruited consecutively from the migraine population attending

Received July 3, 2002; revision received September 3, 2002; accepted September 26, 2002.

From the Neuroimaging Research Unit, Department of Neuroscience (M.A.R., E.P., M.C., M.F.), and Departments of Neurology (B.C., G.C.) and Neuroradiology (A.F., G.S.), Scientific Institute and University Ospedale San Raffaele, Milan, Italy.

Correspondence to Dr Massimo Filippi, Neuroimaging Research Unit Department of Neuroscience, Scientific Institute and University Ospedale San Raffaele, Via Olgettina, 60, 20132 Milan, Italy. E-mail m.filippi@hsr.it

Stroke **is available at http://www.strokeaha.org** **DOI: 10.1161/01.STR.0000057977.06681.11**

TABLE 1. Functional Assessment of Right Upper Limbs From Patients With Migraine and Healthy Volunteers

	Healthy Volunteers	Migraine Patients
Mean time to complete the 9HPT (SD), sec	19.8 (3.2)	20.3 (2.8)
Mean maximum finger tapping rate (SD), sec	3.6 (0.4)	3.5 (0.5)

9HPT indicates 9-hole peg test.

the Outpatient Clinics, Department of Neurology, Scientific Institute and University Ospedale San Raffaele. The diagnosis was established according to the criteria of the Headache Classification Committee of the International Headache Society.[29] To have definite evidence of structural subcortical pathology, the presence of at least 4 brain MRI abnormalities was an additional inclusion criterion. Patients with hypertension, hypercholesteremia, diabetes mellitus, vascular/heart diseases, and other major systemic and neurologic conditions were excluded.

There were 14 women and 1 man; their mean age was 38.0 years (range=16 to 60 years; only 2 patients were older than 50 years, and both of them had evidence of white matter lesions on MRI scans acquired several years before the present study), median disease duration was 15.1 years (range=2 to 40 years), mean number of attacks per year was 26.4 (range=12 to 46), and mean time elapsed from the last attack to the MRI examination was 4.5 weeks (range=2 to 12 weeks). None of them suffered from migraine with aura. At the time MRI was performed, none of the patients was taking any prophylactic treatment for migraine. Fifteen sex- and age-matched right-handed healthy volunteers with no family history of migraine, no previous history of neurological dysfunctions (including migraine), and a normal neurological examination served as controls (13 women and 2 men; mean age=37.3 years, range=26 to 59 years). All subjects were assessed clinically by a single neurologist, who was unaware of the structural and functional MRI results. All migraine patients had a complete normal neurological examination at the time of MRI acquisition. Local Ethical Committee approval and written informed consent from all subjects were obtained before study initiation.

Functional Assessment

Motor functional assessments were performed for all of the subjects at the time of MRI acquisition using the maximum finger-tapping frequency and the 9-hole peg test.[30] Finger-tapping rate and time to complete the 9-hole peg test did not differ between patients and controls (Table 1).

Experimental Design

Using a block design (ABAB), in which 5 periods of activation were alternated with 6 periods of rest (each period of activation and rest consisting of 5 measurements), the subjects were scanned while performing a simple motor task consisting of repetitive flexion-extension of the last 4 fingers of the right hand moving together. The movements were paced by a metronome at a frequency of 1 Hz. Patients and controls were trained before performing the experiments. The subjects were instructed to keep their eyes closed during fMRI acquisition and were monitored visually during scanning to ensure accurate task performance and to check for additional movements.

fMRI Acquisition

Brain MRI scans were obtained using a magnet operating at 1.5 T (Vision, Siemens). Sagittal T_1-weighted images were acquired to define the anterior-posterior commissural (AC-PC) plane. Functional magnetic resonance images were acquired using a T_2*-weighted single-shot echo-planar imaging sequence (TE=66 ms, flip angle=90°, matrix size=128×128, field of view=256×256 mm, TR=3.0 seconds). Twenty-four axial slices parallel to the AC-PC plane and with a thickness of 5 mm, covering the whole brain, were acquired during each measurement. Shimming was performed for the entire brain using an auto-shim routine, which yielded satisfactory magnetic field homogeneity. During each fMRI session, 60 measurements were acquired. The first 5 measurements of each run were discarded to minimize spin saturation effects.

Structural MRI Acquisition

On the same occasion and using the same magnet, the following scans were also obtained: (1) dual-echo turbo spin echo sequence (TR/TE=3300/16–98, echo train length=5) and (2) pulsed-gradient spin-echo (PGSE) echo-planar sequence (interecho spacing=0.8 ms, TE=123 ms), with diffusion gradients applied in 8 noncollinear directions, chosen to cover 3-dimensional space uniformly.[31] The duration and maximal amplitude of the diffusion gradients were, respectively, 25 ms and 21 mT m^{-1}, giving a maximum b factor in each direction of 1044 s mm^{-2}. To optimize the measurement of diffusion, only 2 b factors were used ($b_1 \approx 0$, $b_2=1044$ s mm^{-2}).[32] Fat saturation was performed using a 4-radio frequency–pulse binomial pulse train to avoid the chemical shift artifacts. A birdcage head coil of ≈300 mm in diameter was used for radio frequency transmission and for signal reception. For the turbo spin echo scans, 24 contiguous interleaved axial slices were acquired with 5-mm slice thickness, 256×256 matrix, and 250×250-mm field of view. The slices were positioned to run parallel to a line that joins the most inferoanterior and inferoposterior parts of the corpus callosum.[33] For the PGSE scans, ten axial slices with 5-mm slice thickness, 128×128 matrix, and 250×250-mm field of view were acquired, with the same orientation as the dual-echo scans, with the second-to-last caudal slice positioned to match exactly the central slices of the dual-echo set. This brain portion was chosen because these central slices are less affected by the distortions caused by B_0 field inhomogeneity, which can affect image coregistration.

fMRI Analysis

All image postprocessing was performed offline on a computer workstation (Sun Sparcstation, Sun Microsystems). fMRI data were analyzed using the statistical parametric mapping (SPM99) software developed by Friston et al.[34] Before statistical analysis, all images were realigned to the first one to correct for subject motion, spatially normalized into SPM standard space, and smoothed with a 10-mm, 3-dimensional gaussian filter. Changes in blood oxygenation level–dependent (BOLD) contrast associated with the performance of the motor task were assessed on a pixel-by-pixel basis, using the general linear model[34] and the theory of gaussian fields.[35] Specific effects were tested by applying appropriate linear contrasts. Significant hemodynamic changes for each contrast were assessed using t statistical parametric maps on a voxel-by-voxel basis. We limited our analysis to a group of a priori–selected cortical areas (ipsi- and contralateral primary sensorimotor cortex [SMC], supplementary motor area [SMA], and ipsi- and contralateral secondary somatosensory cortex [SII]),[36] because these areas are known to be activated during the performance of simple motor tasks, as previously shown by studies based either on a region-of-interest analysis (ROI)[19–21] or on a more rigid voxel-based analysis.[22–25] Only those clusters that showed a significant activation at a threshold of $P<0.05$ corrected for multiple comparisons ($t<5.3$) were considered in this analysis. For each cluster, we measured the spatial extent of the activation and the coordinates of the centers of activations. In each subject, the mean time course of the signal intensity change in each of the clusters was also calculated, by averaging over the 5 cycles of rest and task performance. From these time courses a mean curve for each cluster was obtained for migraine patients and healthy volunteers to assess whether any difference in the shape of curves between the 2 groups could be detected.

Structural MRI Postprocessing

All of the structural MRI analysis was performed by a single experienced observer who was unaware to whom the scans belonged and blinded to the fMRI results. Lesions were identified on the proton density–weighted scans (T_2-weighted images were always used to increase confidence in lesion identification), and lesion

TABLE 2. Mean (SD) $\bar{D}$ Histogram-Derived Metrics of NAWM From Healthy Volunteers and Patients With Migraine

	Healthy Volunteers	Migraine Patients	P*
NAWM average $\bar{D}$ (SD), $\times 10^{-3}$ mm^2 s^{-1}	0.78 (0.01)	0.79 (0.02)	ns
NAWM mean $\bar{D}$ histogram peak height (SD)	211.8 (22.8)	194.0 (14.2)	0.02
NAWM mean $\bar{D}$ histogram peak position (SD), $\times 10^{-3}$ mm^2 s^{-1}	0.73 (0.01)	0.73 (0.03)	ns

*For statistical analysis, see text.

NAWM indicates normal appearing white matter; SD, standard deviation; ns, not significant.

volumes were measured using a segmentation technique based on local thresholding, as previously described.[37] PGSE images were first corrected for geometrical distortion induced by eddy currents using an algorithm that maximizes mutual information between the diffusion unweighted and weighted images.[38] Then, the DT was calculated and mean diffusivity ($\bar{D}$) and fractional anisotropy (FA) were derived for every pixel, as previously described.[39] The diffusion images were interpolated to the same image matrix size as the dual-echo images, and then the $b=0$ step of the PGSE scans (T_2 weighted but not diffusion weighted) was coregistered with the dual-echo T_2-weighted images using a 3-dimensional rigid-body coregistration algorithm based on mutual information.[38] The final step consisted of automatic transfer of lesion outlines onto the $\bar{D}$ maps and calculation of average lesion $\bar{D}$ and FA. To study the $\bar{D}$ of NAWM, pixels lying inside lesion outlines were nulled out, and $\bar{D}$ histograms of the remaining NAWM were produced, as previously described.[39] To correct for the between-subject differences in brain volume, each histogram was normalized by dividing the height of each bin by the total number of pixels contributing to the histogram. For each histogram, the following measures were derived: the relative peak height (ie, the proportion of pixels at the most common $\bar{D}$ value), the peak location (ie, the most common $\bar{D}$ value), and the average $\bar{D}$.

Statistical Analysis

To test between-group differences in spatial extent and centers of activations of the fMRI clusters, a 2-tailed Student *t* test for nonpaired data was used. The same test was also used to compare NAWM $\bar{D}$ histogram–derived metrics from migraine patients and controls. To assess the correlation of BOLD changes with structural MRI findings in migraine patients, structural metrics were entered into the SPM design matrix, using basic models and linear regression analysis.[40]

Results

All healthy volunteers had normal brain MRI dual-echo scans. In patients with migraine, the median dual-echo lesion load was 0.7 mL (range=0.1 to 14.6 mL), average lesion $\bar{D}$ was 0.86×10^{-3} mm^2 s^{-1} (SD=0.06×10^{-3} mm^2 s^{-1}) and average lesion FA was 0.26 (SD=0.05). None of the lesions from patients with migraine was located along the brain pyramidal tracts. In Table 2, $\bar{D}$ histogram–derived metrics of the NAWM from healthy subjects and migraine patients are shown. Migraine patients had significantly lower $\bar{D}$ histogram peak height of the NAWM in comparison with healthy subjects.

During fMRI acquisition, all subjects performed the task correctly and no additional movements were noted. In Table 3, the mean cluster sizes of the activated brain areas at individual subject analysis, and the coordinates of the centers of activations are presented for healthy volunteers and migraine patients. Compared with healthy volunteers, migraine patients had a larger relative activation of the contralateral primary SMC ($P=0.01$) (Table 3 and Figure 1), and a rostral displacement of the SMA ($P=0.03$) (Table 3, Figure 1). The shapes of the curves reflecting the time course for BOLD signal intensity changes were similar between migraine patients and controls for all of the a priori–selected cortical areas. In Figure 2, the time courses for the contralateral SMC signal intensity changes in healthy volunteers and migraine patients are shown.

The peak height of the NAWM $\bar{D}$ histogram was correlated with the extent of rostral displacement of the SMA ($r=-0.80$, $P<0.001$) (Figure 3). No correlations were found between fMRI changes and any of the structural MR metrics quantifying the extent and the severity of the intrinsic damage of lesions visible on dual-echo scans.

TABLE 3. Spatial Extents and Coordinates of the Centers of Activation of the Cortical Areas Studied in Healthy Volunteers and Patients With Migraine

	Mean Cluster Sizes (SD)		Standard Space Coordinates	
			Healthy Volunteers	Migraine Patients
	Healthy Volunteers	Migraine Patients	X Y Z	X Y Z
R SMC	335.8 (655.2)	808.6 (908.7)	41, −37, 51	37, −35, 49
L SMC	1719.0 (980.5)	3252.1 (1836.3)*	−36, −18, 60	−36, −24, 61
Bilateral SMA	281.3 (209.1)	336.8 (153.6)	−2, −6, 53	−2, −3, 60*
R SII	223.2 (132.9)	160.8 (147.5)	61, −18, 15	61, −17, 16
L SII	235.1 (284.9)	370.5 (369.4)	−57, −24, 15	−54, −28, 15

*Statistically significant differences (2-tailed Student *t* test for nonpaired data). See text for further details.

R indicates right; L, left; SMC, sensorimotor cortex; SMA, supplementary motor area; SII, secondary somatosensory cortex (upper bank of sylvian fissure); SD, standard deviation.

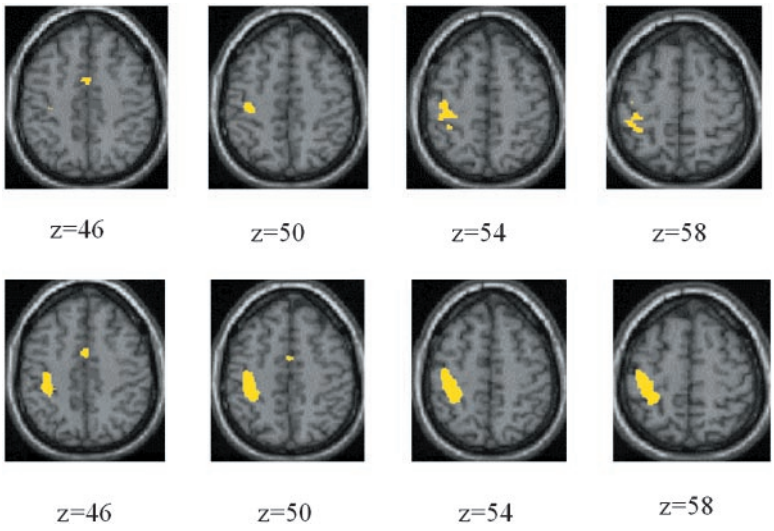

Figure 1. Different patterns of cortical activations during performance of a simple motor task with functionally normal upper right limbs in right-handed healthy volunteers (top row) and patients with migraine (bottom row). A greater activation of the contralateral primary SMC and a rostral displacement of the SMA are visible in patients with migraine.

Discussion

During the past decade, fMRI has widely been applied to elucidate the role of cortical reorganization after brain injury.[16–25] Cortical adaptive changes have been demonstrated in several neurological conditions, including stroke,[16,17] tumors,[18] and MS.[19–25] A recent study[41] has shown dramatic fMRI changes in the visual cortex of patients experiencing migraine aura, but, to our knowledge, there are no fMRI studies investigating whether interictal cortical reorganization occurs in patients with migraine and whether this is correlated with the extent of subcortical white matter damage. To this end, we selected only migraine patients with evidence of structural subcortical pathology. As a consequence, the results of this study cannot be generalized to the overall population of patients with migraine, but should rather be interpreted as an additional piece of evidence that functional cortical reorganization occurs even in the presence of relatively mild white matter structural abnormalities.[24] The fact that the patients studied had no neurological symptoms or signs and performed a simple motor task with a fully normal upper limb removes the potential confounding factors of performance differences.

This study showed that the pattern of movement-related cortical activations is different between migraine patients with dual-echo hyperintense lesions on brain MRI scans and matched healthy volunteers. When contrasted to controls, patients with migraine had increased contralateral SMC activation and a shift of the center of SMA activation, suggesting that migraine can be associated with local functional reorganization of the cortex outside the cephalalgic phase of the disease. Functionally, the SMA can be divided into a pre-SMA (located more rostrally) and a SMA proper (located more caudally), and previous event-related fMRI studies have shown the pre-SMA to be preferentially activated in movement preparation.[42,43] In addition, recent work

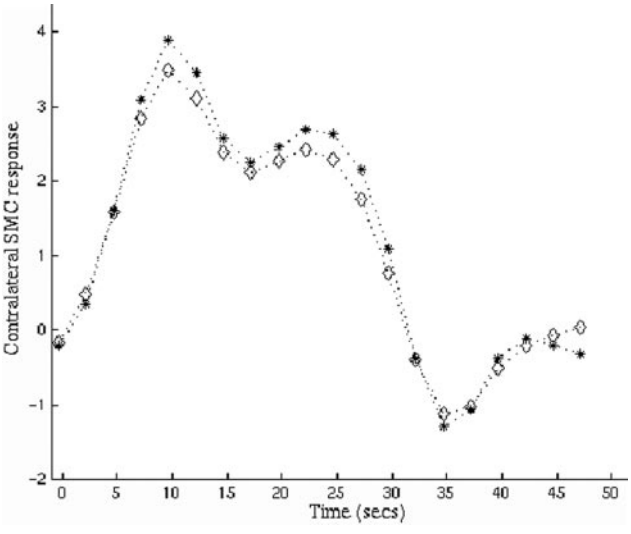

Figure 2. Time courses for the contralateral primary SMC BOLD signal intensity changes in healthy volunteers (*) and patients with migraine (◇). The shape of the curve and the signal intensity changes were similar between healthy volunteers and migraine patients.

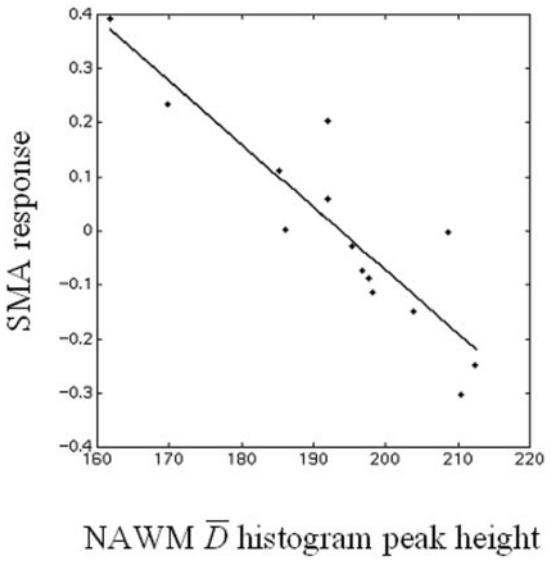

Figure 3. Correlation between relative activation of the SMA and NAWM $\bar{D}$ histogram peak height.

has also shown that rostral SMA activation precedes primary motor cortex activation by several seconds.[44] Thus, the rostral displacement of the SMA detected in patients with migraine might be secondary to an increased activation of the pre-SMA in these patients. Increased activation of the pre-SMA might be the reflection of patients' perception of the task as relatively difficult (given the presence of widespread white matter damage) and might, in turn, cause a greater SMC activation through fibers connecting these 2 cortical areas, via the SMA proper.[45] The increased SMC activation might then lead to an increased recruitment of corticospinal fibers projecting from this area[46,47] to maintain a normal level of functioning in the presence of structural brain damage. This interpretation of the results also fits with the notion that increased SMA and SMC activations can be seen in healthy subjects during the performance of complex motor tasks.[48,49]

Migraine patients were selected to have evidence of subcortical tissue damage on dual-echo scans to assess whether any relationship exists between structural damage and cortical fMRI changes. We also obtained DT-MRI of the brain from our patients to assess, in addition to lesion extent, the severity of tissue damage within and outside macroscopic white matter lesions. DT-MRI can provide quantitative information about size, shape, orientation, and geometry of water-filled spaces in the brain,[50] and recent work has shown its exquisite sensitivity in detecting tissue changes beyond the resolution of conventional MRI in the white matter of patients with ischemic conditions, such as CADASIL[26] and leukoaraiosis.[28] We found a reduction of the peak height of the NAWM $\bar{D}$ histograms in migraine patients compared with controls. Because the peak height of the $\bar{D}$ histogram is considered to be a measure of the residual amount of truly normal tissue[39] and we included in this analysis all the pixels belonging to NAWM, our results indicate that damage of white matter in migraine is not confined to those areas that appear abnormal on dual-echo scans, but includes more subtle changes in NAWM. Even more interestingly, we found a direct relationship between the extent of the shift of the center of activation of SMA and the peak height of the NAWM $\bar{D}$ histograms. This suggests that changes in brain function may be induced by the extent of diffuse NAWM damage, which, by impairing physiological cross talk between cortical areas involved in the widespread movement-associated network of the human brain,[46,47] might result in patients' perception of this simple task as a more complex task,[48,49] thus requiring increased recruitment of neurons in the SMC and in the rostral part of the SMA. In this respect, it might be worth noting that patients with nondisabling relapsing-remitting MS, who have relatively few dual-echo hyperintense lesions and a diffuse NAWM involvement (such as the migraine patients we studied), also show increased contralateral SMC activation and a correlation between the extent of NAWM damage and the extent of SMA activation, when performing the same motor task.[24] Although this study cannot respond to the question of whether functional cortical reorganization in such patients contributes to the absence of neurological impairment and disability, despite the presence of subcortical damage, this is an intriguing issue that deserves to be investigated by future longitudinal studies.

The pathologic substrate of NAWM changes in patients with migraine remains unknown, and definitive histopathologic correlations in these patients are unlikely to be obtained. Nevertheless, at least 2 possible explanations for reduced peak height of the NAWM $\bar{D}$ histogram are readily apparent. First, DT-MRI changes in NAWM could result from ischemia caused by the blood flow reduction, which can persist for hours during a migraine attack.[14] Alternatively, changes could reflect secondary wallerian degeneration of axons projecting into the NAWM from damaged tissue.

The BOLD response includes contributions from multiple factors, including increased blood flow and an increase in blood volume in cortical tissue in addition to effects of an increase in the proportion of the oxygenated relative to deoxygenated hemoglobin.[51,52] Because it has been postulated that dysbalance of the cerebrovascular response during functional activation of the brain may be a factor in migraine pathophysiology,[53,54] we investigated whether the time course of the hemodynamic response in the a priori–selected cortical areas was different between patients and healthy volunteers. We found no difference in the time course of the BOLD signal intensity changes in all of the areas we studied between patients and controls, and, as a consequence, this suggests that the changes in cortical activation seen in the present study are more likely attributable to cortical reorganization secondary to diffuse white matter damage rather than to cortical perfusion abnormalities known to occur in patients with migraine.[53,54]

References

1. Ferbert A, Busse D, Thron A. Microinfarction in classic migraine? A study with magnetic resonance imaging findings. *Stroke*. 1991;22:1010–1014.
2. Igarashi H, Sakai F, Kan S, Okada J, Tazaky Y. Magnetic resonance imaging of the brain in patients with migraine. *Cephalalgia*. 1991;11:69–74.
3. Osborn RE, Alder DC, Mitchell CS. MR imaging of the brain in patients with migraine headaches. *AJNR Am J Neuroradiol*. 1991;12:521–524.
4. Ziegler DK, Batnitzky S, Barter R, McMillan JH. Magnetic resonance image abnormality in migraine with aura. *Cephalalgia*. 1991;11:147–150.
5. Fazekas F, Koch M, Schmidt R, Offenbacher H, Payer F, Freidl W, Lechner H. The prevalence of cerebral damage varies with migraine type: a MRI study. *Headache*. 1992;32:287–291.
6. Robbins L, Friedman H. MRI in migraineurs. *Headache*. 1992;32:507–508.
7. Pavese N, Canapicchi R, Nuti A, Bibbiani F, Lucetti C, Collavoli P, Bonuccelli U. White matter MRI hyperintensities in a hundred and twenty-nine consecutive migraine patients. *Cephalalgia*. 1994;14:342–345.
8. De Benedettis G, Lorenzetti A, Sina C, Bernasconi V. Magnetic resonance imaging in migraine and tension-type headache. *Headache*. 1995;35:264–268.
9. Cooney BS, Grossman RI, Farber RE, Goin JE, Galetta SL. Frequency of magnetic resonance imaging abnormalities in patients with migraine. *Headache*. 1996;36:616–621.
10. Fazekas F, Barkhof F, Filippi M. Unenhanced and enhanced magnetic resonance imaging in the diagnosis of multiple sclerosis. *J Neurol Neurosurg Psychiatry*. 1998;64:S2–S5.
11. Rocca MA, Colombo B, Pratesi A, Comi G, Filippi M. A magnetization transfer imaging study of the brain in patients with migraine. *Neurology*. 2000;54:507–509.
12. Olesen J, Larsen B, Lauritzen M. Focal hyperemia followed by spreading oligemia and impaired activation of rCBF in classic migraine. *Ann Neurol*. 1981;9:344–352.
13. Olesen TS, Friberg L, Lassen NA. Ischemia may be the primary cause of the neurologic deficits in classic migraine. *Arch Neurol*. 1987;44:156–161.

14. Olesen J, Friberg L, Olsen TS, Iversen HK, Lassen NA, Andersen AR, Karle A. Timing and topography of cerebral blood flow, aura, and headache during migraine attacks. *Ann Neurol*. 1990;28:791–798.
15. Friberg L, Olesen J, Lassen NA, Olesen TS, Karle A. Cerebral oxygen extraction, oxygen consumption and regional cerebral blood flow during the aura phase of migraine. *Stroke*. 1994;25:974–979.
16. Cramer SC, Nelles G, Benson RR, Kaplan JD, Parker RA, Kwong KK, Kennedy DN, Finklestein SP, Rosen BR. A functional MRI study of subjects recovered from hemiparetic stroke. *Stroke*. 1997;28:2518–2527.
17. Cao Y, D'Olhaberriague L, Vikingstad EM, Levine SR, Welch KM. Pilot study of functional MRI to assess cerebral activation of motor function after poststroke hemiparesis. *Stroke*. 1998;29:112–122.
18. Fandino J, Kollias SS, Wieser HG, Valavanis A, Yonekawa Y. Intraoperative validation of functional magnetic resonance imaging and cortical reorganization patterns in patients with brain tumors involving the primary motor cortex. *J Neurosurg*. 1999;91:238–250.
19. Lee M, Reddy H, Johansen-Berg H, Pendlebury S, Jenkinson M, Smith S, Palace J, Matthews PM. The motor cortex shows adaptive functional changes to brain injury from multiple sclerosis. *Ann Neurol*. 2000;47: 606–613.
20. Reddy H, Narayanan S, Arnoutelis R, Jenkinson M, Antel J, Matthews PM, Arnold DL. Evidence for adaptive functional changes in the cerebral cortex with axonal injury from multiple sclerosis. *Brain*. 2000;123: 2314–2320.
21. Reddy H, Narayanan S, Matthews PM, Hoge RD, Pike GB, Duquette P, Antel J, Arnold DL. Relating axonal injury to functional recovery in MS. *Neurology*. 2000;54:236–239.
22. Filippi M, Rocca MA, Colombo B, Falini A, Codella M, Scotti G, Comi G. Functional magnetic resonance imaging correlates of fatigue in multiple sclerosis. *Neuroimage*. 2002;15:559567.
23. Filippi M, Rocca MA, Falini A, Caputo D, Ghezzi A, Colombo B, Scotti G, Comi G. Correlations between structural CNS damage and functional MRI changes in primary progressive MS. *Neuroimage*. 2002;15:537–546.
24. Rocca MA, Falini A, Colombo B, Scotti G, Comi G, Filippi M. Adaptive functional changes in the cerebral cortex of patients with non-disabling MS correlate with the extent of brain structural damage. *Ann Neurol*. 2002;51:330–339.
25. Rocca MA, Matthews PM, Caputo D, Ghezzi A, Falini A, Scotti G, Comi G, Filippi M. Evidence for widespread movement-associated functional MRI changes in patients with PPMS. *Neurology*. 2002;58:866–872.
26. Chabriat H, Pappata S, Poupon C, Clark CA, Vahedi K, Poupon F, Mangin JF, Pachot-Clouard M, Jobert A, Le Bihan D, Bousser MG. Clinical severity in CADASIL related to ultrastructural damage in white matter: in vivo study with diffusion tensor MRI. *Stroke*. 1999;30: 2637–2643.
27. Filippi M. In-vivo tissue characterization of multiple sclerosis and other white matter diseases using magnetic resonance based techniques. *J Neurol*. 2001;248:1019–1029.
28. O'Sullivan M, Summers PE, Jones DK, Jarosz JM, Williams SC, Markus HS. Normal-appearing white matter in ischemic leukoaraiosis: a diffusion tensor MRI study. *Neurology*. 2001;57:2307–2310.
29. Headache Classification Committee of the International Headache Society: Proposed classification and diagnostic criteria for headache disorders, cranial neuralgias and facial pain. *Cephalalgia*. 1988;8(suppl 7):1–96.
30. Herndon RM. Handbook of Neurologic Rating Scales. New York: Demos Vermande; 1997.
31. Jones DK, Horsfield MA, Simmons A. Optimal strategies for measuring diffusion in anisotropic systems by magnetic resonance imaging. *Magn Reson Med*. 1999;42:515–525.
32. Bito Y, Hirata S, Yamamoto E. Optimal gradient factors for ADC measurements. *Proc Intl Soc Magn Reson Med*. 1995;2:913.
33. Miller DH, Barkhof F, Berry I, Kappos L, Scotti G, Thompson AJ. Magnetic resonance imaging in monitoring the treatment of multiple sclerosis: Concerted Action Guidelines. *J Neurol Neurosurg Psychiatry*. 1991;54:683–688.
34. Friston KJ, Holmes AP, Poline JB, Grasby PJ, Williams SC, Frackowiak RS, Turner R. Analysis of fMRI time-series revisited. *Neuroimage*. 1995; 2:45–53.
35. Worsley KJ, Friston KJ. Analysis of fMRI time-series revisited again. *Neuroimage*. 1995;2:173–181.
36. Poline JB, Worsley KJ, Evans AC, Friston KJ. Combining spatial extent and peak intensity to test for activations in functional imaging. *Neuroimage*. 1997;5:83–96.
37. Rovaris M, Filippi M, Calori G, Rodegher M, Campi A, Colombo B, Comi G. Intra-observer reproducibility in measuring new putative MR markers of demyelination and axonal loss in multiple sclerosis: a comparison with conventional T2-weighted images. *J Neurol*. 1997;244: 266–270.
38. Studholme C, Hill DLG, Hawkes DJ. Automated three-dimensional registration of magnetic resonance and positron emission tomography brain images by multiresolution optimization of voxel similarity measures. *Med Phys*. 1996;24:25–35.
39. Cercignani M, Inglese M, Pagani E, Comi G, Filippi M. Mean diffusivity and fractional anisotropy histograms of patients with multiple sclerosis. *AJNR Am J Neuroradiol*. 2001;22:952–958.
40. Friston KJ, Holmes AP, Price CJ, Buchel C, Worsley KJ. Multisubject fMRI studies and conjunction analyses. *Neuroimage*. 1999;10:385–396.
41. Hadjikhani N, Sanchez Del Rio M, Wu O, Schwartz D, Bakker D, Fischl B, Kwong KK, Cutrer FM, Rosen BR, Tootell RB, Sorensen AG, Moskowitz MA. Mechanisms of migraine aura revealed by functional MRI in human visual cortex. *Proc Natl Acad Sci U S A*. 2001;98:4687–4692.
42. Humberstone M, Sawle GV, Clare S, Hykin J, Coxon R, Bowtell R, Macdonald IA, Morris PG. Functional magnetic resonance imaging of single motor events reveals human presupplementary motor area. *Ann Neurol*. 1997;42:632–637.
43. Lee KM, Chang KH, Roh JK. Subregions within the supplementary motor area activated at different stages of movement preparation and execution. *Neuroimage*. 1999;9:117–123.
44. Weilke F, Spiegel S, Boecker H, von Einsiedel HG, Conrad B, Schwaiger M, Erhard P. Time-resolved fMRI of activation patterns in M1 and SMA during complex voluntary movement. *J Neurophysiol*. 2001;85: 1858–1863.
45. Luppino G, Matelli M, Camarda R, Rizzolatti G. Corticocortical connections of area F3 (SMA-proper) and area F6 (pre-SMA) in the macaque monkey. *J Comp Neurol*. 1993;338:114–140.
46. Martino AM, Strick PL. Corticospinal projections originate from the arcuate premotor area. *Brain Res*. 1987;404:307–312.
47. Jacobs KM, Donoghue JP. Reshaping the cortical motor map by unmasking latent intracortical connections. *Science*. 1991;251:944–947.
48. Weilke F, Spiegel S, Boecker H, von Einsiedel HG, Conrad B, Schwaiger M, Erhard P. Time-resolved fMRI of activation patterns in M1 and SMA during complex voluntary movement. *J Neurophysiol*. 2001;85: 1858–1863.
49. Shibasaki H, Sadato N, Lyshkow H, Yonekura Y, Honda M, Nagamine T, Suwazono S, Magata Y, Ikeda A, Miyazaki M. Both primary motor cortex and supplementary motor area play an important role in complex finger movement. *Brain*. 1993;116:1387–1398.
50. Le Bihan D, Turner R, Pekar J, Moonen CTW. Diffusion and perfusion imaging by gradient sensitization: design, strategy and significance. *J Magn Reson Imaging*. 1991;1:7–8.
51. Ogawa S, Lee TM, Kay AR, Tank DW. Brain magnetic resonance imaging with contrast dependent on blood oxygenation. *Proc Natl Acad Sci U S A*. 1990;87:9868–9872.
52. Buxton RB, Frank LR. A model for the coupling between cerebral blood flow and oxygen metabolism during neural stimulation. *J Cereb Blood Flow Metab*. 1997;17:64–72.
53. Thie A, Carvajal-Lizano M, Schlichting U, Spitzer K, Kunze K. Multimodal tests of cerebrovascular reactivity in migraine: a transcranial Doppler study. *J Neurol*. 1992;239:338–342.
54. Backer M, Sander D, Hammes MG, Funke D, Deppe M, Conrad B, Tolle TR. Altered cerebrovascular response pattern in interictal migraine during visual stimulation. *Cephalalgia*. 2001;21:611–616.

Evidence for Cortical Functional Changes in Patients With Migraine and White Matter Abnormalities on Conventional and Diffusion Tensor Magnetic Resonance Imaging

Maria A. Rocca, Bruno Colombo, Elisabetta Pagani, Andrea Falini, Maria Codella, Giuseppe Scotti, Giancarlo Comi and Massimo Filippi

Stroke. 2003;34:665-670; originally published online February 13, 2003;
doi: 10.1161/01.STR.0000057977.06681.11
Stroke is published by the American Heart Association, 7272 Greenville Avenue, Dallas, TX 75231

Print ISSN: 0039-2499. Online ISSN: 1524-4628